JOURNAL OF GUIDANCE, CONTROL, AND DYNAMICS
Vol. 26, No. 4, July–August 2003

Invariant Manifold Tracking for First-Order Nonlinear Hill's Equations

Jason W. Mitchell*
Air Force Research Laboratory, Wright–Patterson Air Force Base, Ohio 45433
and
David L. Richardson†
University of Cincinnati, Cincinnati, Ohio 45221

An approach to provide nonlinear active control for first-order nonlinear classical Hill's equations is described. Both linearized and nonlinear Hill's equations are controlled to remain close to specific invariant manifolds defined through the various system Hamiltonians. It is then shown that trajectories similar to the periodic trajectories of the linearized system can be maintained by the nonlinear equations on invariant manifolds defined by the linearized system of equations. Forcing the nonlinear system trajectories onto an invariant manifold of the linearized system, with an appropriate choice of initial conditions, provides a significant reduction in the along-track drift of first-order nonlinear Hill's equations as compared to linearized equations. There is also a small drift reduction in the radial coordinate direction. The cross-track position suffers only a slight increase in the maximum amplitude of its oscillation.

Introduction

INCREASED interest in multiple-satellite formation flight is driving the development of control schemes to provide efficient formation keeping.[1–3] Often, these investigations rely on the Clohessy–Wiltshire equations,[4] that is, linearized Hill's equations,[5] to describe the relative motion of satellites in nearly circular orbits. With first-order nonlinear Hill's equations, as is frequently the case outside linear system theory, major hurdles in control system design include determining the form of the control and when control should be applied. These difficulties are particularly severe in the control of artificial satellites where control authority is fuel limited, and fuel availability is restricted by launch weight. All of this is exacerbated by perturbations due to the Earth's gravitational field, drag, solar radiation pressure, and third-body effects. Such disturbances significantly impact the evolution of the system's dynamics. Fortunately, it is frequently possible to mine the continuous system dynamics, governed by differential-algebraic equations, for additional information to enhance the control system design.

Because linearized models cannot provide a complete description of relative motion, we elected to explore the dynamics and control of the nonlinear Hill's system by including first-order nonlinear effects in addition to those generated by the linear equations. The effects of the asphericity of the Earth play a central role in the design of control schemes for long-term formation keeping. These effects are similar in magnitude to those nonlinear contributions considered herein, and so an analysis of nonlinear Hill's effects on the motion and control dynamics was deemed appropriate.

In the present paper, we investigate the dynamic properties of the linearized and first-order nonlinear Hill's equations to control relative satellite motion described by the first-order nonlinear Hill's equations using a modification of a scheme first presented by Baumgarte.[6] We begin with a brief review of Hill's equations.

Received 7 November 2000; revision received 28 February 2003; accepted for publication 8 March 2003.

*Visiting Scientist, Air Vehicles Directorate, Control Theory Optimization Branch (VACA), 2210 8th Street. Member AIAA.

†Professor, Aerospace Engineering and Engineering Mechanics, P.O. Box 210070.

First-Order Nonlinear Hill's Equations

Consider two small satellites, a leader and a follower satellite, in a drag-free orbit about a spherical central body. Because each satellite experiences only the central force field of the central body, the individual satellite accelerations are given by

$$\ddot{\boldsymbol{r}}_i = -\left(\mu/r_i^3\right)\boldsymbol{r}_i \tag{1}$$

where the subscript i indicates each satellite's index: 0 for the leader satellite and 1 or higher for additional follower satellites. Positions relative to the circular orbiting leader satellite for $i > 0$ are written as

$$\boldsymbol{\rho}_i = \boldsymbol{r}_i - \boldsymbol{r}_0 = X_i\hat{\boldsymbol{e}}_x + Y_i\hat{\boldsymbol{e}}_y + Z_i\hat{\boldsymbol{e}}_z \tag{2}$$

where, as with Hill's notation, $\hat{\boldsymbol{e}}_x$, $\hat{\boldsymbol{e}}_y$, and $\hat{\boldsymbol{e}}_z$ form a local dextral system of coordinates with origin at the leader as seen in Fig. 1. The $\hat{\boldsymbol{e}}_x$ axis lies in the direction of the radial line outward from the central body (Earth), $\hat{\boldsymbol{e}}_y$ is oriented in the along-track (instantaneous velocity) direction, and $\hat{\boldsymbol{e}}_z$ lies along the orbit normal in the direction of the angular momentum vector.

When we differentiate Eq. (2), the relative follower accelerations are given by

$$\ddot{\boldsymbol{\rho}}_i = \left(\mu/r_0^3\right)\left[\boldsymbol{r}_0 - \left(r_0^2/r_i^3\right)\boldsymbol{r}_i\right] \tag{3}$$

Taking $i = 1$ and dropping that subscript, for $\boldsymbol{r} = \boldsymbol{r}_0 + \boldsymbol{\rho}$, we have

$$\boldsymbol{r}/r^3 = \left[(\boldsymbol{r}_0 + \boldsymbol{\rho})/r_0^3\right]\left(1 - \tfrac{3}{2}\left\{\left[2(\boldsymbol{r}_0 \cdot \boldsymbol{\rho}) + \rho^2\right]/r_0^2\right\} + \tfrac{15}{8}\left[2(\boldsymbol{r}_0 \cdot \boldsymbol{\rho})/r_0^2\right]^2 + \mathcal{O}(\rho^3)\right) \tag{4}$$

To complete the algebra, we substitute Eq. (4) into Eq. (3), neglect terms of $\mathcal{O}(\rho^3)$, and equate the result to the acceleration of the rotating frame while noting that the frame's rate $n = \sqrt{(\mu/r_0^3)}$ is constant. In addition, we nondimensionalize the length scale and timescale by the leader's circular orbit radius r_0 and mean motion n, respectively, such that $\boldsymbol{\rho}/r_0 = [X \;\; Y \;\; Z]^T/r_0 = [x \;\; y \;\; z]^T$ and $\tau = nt$. Thus, including first-order nonlinear terms in Hill's equations, using the notation $(') = \mathrm{d}/\mathrm{d}\tau$ for differentiation, results in the system of equations given by

$$x'' - 2y' - 3x = -\tfrac{3}{2}(2x^2 - y^2 - z^2) \tag{5a}$$

$$y'' + 2x' = 3xy \tag{5b}$$

$$z'' + z = 3xz \tag{5c}$$

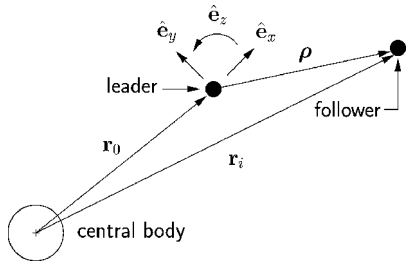

Fig. 1 Leader–follower geometry with $\hat{e}_x \times \hat{e}_y = \hat{e}_z$.

which can be obtained from the Lagrangian

$$\mathcal{L} = \tfrac{1}{2}(x'^2 + y'^2 + z'^2) + (xy' - yx') + \tfrac{1}{2}(3x^2 - z^2) - \tfrac{1}{2}(2x^3 - 3xy^2 - 3xz^2) \tag{6}$$

Linearized Hill's Equations

By taking zero right-hand sides of Eqs. (5), we obtain the nondimensional, drag-free, linearized Hill's equations[7] describing the motion of a follower satellite relative to a circular-orbiting, and possibly fictitious, leader satellite,

$$x'' - 2y' - 3x = 0 \tag{7a}$$

$$y'' + 2x' = 0 \tag{7b}$$

$$z'' + z = 0 \tag{7c}$$

Equations (7) can be obtained from the Lagrangian

$$\mathcal{L} = \tfrac{1}{2}(x'^2 + y'^2 + z'^2) + (xy' - yx') + \tfrac{1}{2}(3x^2 - z^2) \tag{8}$$

and admit an analytical solution given by

$$x(\tau) = -\tfrac{2}{3}A_2 + \tfrac{1}{2}(A_4 \cos\tau + A_3 \sin\tau) \tag{9a}$$

$$y(\tau) = A_1 + A_2\tau + A_3 \cos\tau - A_4 \sin\tau \tag{9b}$$

$$z(\tau) = A_5 \cos\tau + A_6 \sin\tau \tag{9c}$$

When it is known that the parameters A_i, $i = 1, 6$, are related to the initial conditions by

$$A_1 = y_0 - 2x_0' \tag{10a}$$

$$A_2 = -3(2x_0 + y_0') \tag{10b}$$

$$A_3 = 2x_0' \tag{10c}$$

$$A_4 = -2(3x_0 + 2y_0') \tag{10d}$$

$$A_5 = z_0 \tag{10e}$$

$$A_6 = z_0' \tag{10f}$$

it is clear from Eqs. (9) that periodic solutions are obtained by requiring

$$A_2 = -3(2x_0 + y_0') = 0 \tag{11}$$

which reduces to the condition

$$y_0' = -2x_0 \tag{12}$$

The resulting periodic trajectories about the leader satellite are highly desirable for formation-keeping considerations.

Table 1 Initial conditions

Position	km	Rate	km/s
X_0	0.500	X_0'	0.000
Y_0	0.000	y_0'	$-2x_0$
Z_0	0.050	Z_0'	0.000

Table 2 Comparison of linear to uncontrolled first-order nonlinear dynamics for one day

q	$\|q\|_2$	$\|q\|_\infty$
$\Delta X_{\ell n}$, m	1.944 284e+00	8.166 285e−02
$\Delta Y_{\ell n}$, m	9.865 215e+01	5.425 019e+00
$\Delta Z_{\ell n}$, m	1.954 143e−01	8.207 369e−03
$\Delta X'_{\ell n}$, m/s	1.267 349e−03	7.070 782e−05
$\Delta Y'_{\ell n}$, m/s	2.648 508e−03	1.600 963e−04
$\Delta Z'_{\ell n}$, m/s	1.273 716e−04	7.106 087e−06

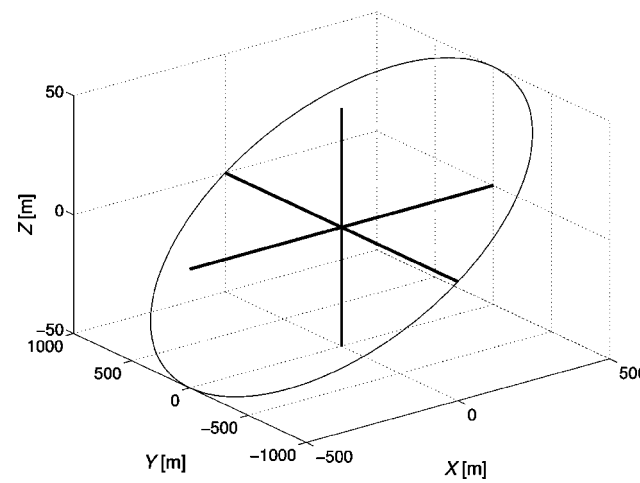

Fig. 2 Follower positions relative the leader for approximately one day using linear Hill's equations.

Comparing the Linearized and Nonlinear Motion

When we choose a nominal altitude of 500 km and an initial separation of 500 m radially above the leader satellite, that is, $y_0 = 0$, along with a cross-track separation of 50 m, $x_0' = z_0' = 0$, and y_0' given by Eq. (12), the relative position for the duration of approximately one day (nearly 16 orbit revolutions) can be seen in Fig. 2. This trajectory is desirable because it is configuration preserving.

The first-order nonlinear terms in Eqs. (5) produce nonnegligible drifts in the along-track and radial directions, as well as their rates. The resulting trajectories about the leader satellite are no longer the highly desirable periodic trajectories produced by linearized Hill's equations (7) subject to the condition given by Eq. (12). When we use the same initial conditions as for the linearized system (Table 1), the nonlinear positions initially appear to be identical to Fig. 2. On closer inspection, we see a difference in positions and rates for the same periodic initial conditions as demonstrated by Figs. 3–5 and Table 2. The nonlinear solution's radial ($\Delta X_{\ell n}$) and cross-track ($\Delta Z_{\ell n}$) deviations from the periodic linear solution are several orders of magnitude smaller than the along-track error that is introduced. In the along-track case, the follower satellite advances on the leader satellite by more than 5 m/day. This drift is the same order of magnitude as that produced by drag at 500 m in altitude and accordingly is a significant contribution to formation-keeping considerations.

When we consider the many differences among force model descriptions for the motion, it is convenient to obtain a mechanism that can accommodate an increase in model fidelity while allowing the improved system to be controlled so that the resulting (nonlinear) trajectories can be made very similar to that of the periodic linear solutions. In the sequel, we apply and test a scheme to provide

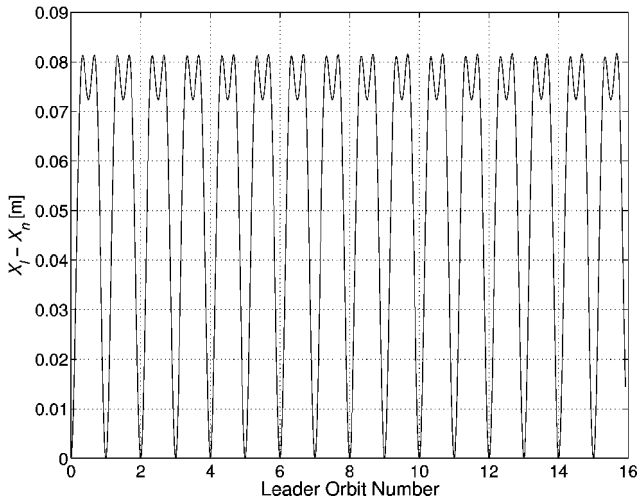

Fig. 3 Radial position difference between linear and nonlinear Hill's equations.

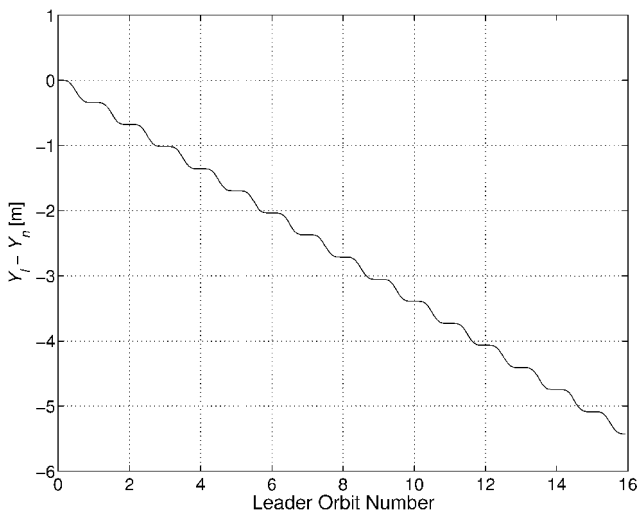

Fig. 4 Along-track position difference between the linear and nonlinear Hill's equations.

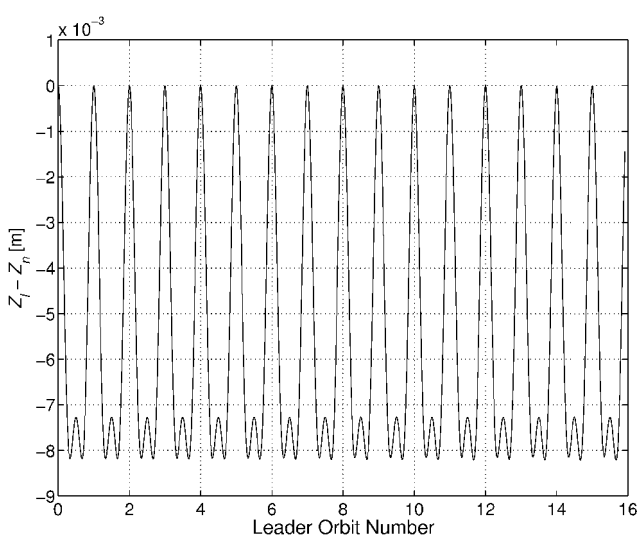

Fig. 5 Cross-track position difference between the linear and nonlinear Hill's equations.

such control stemming only from the dominant contributions arising from the nonlinear Hill's equations. Our purpose here is to demonstrate control considerations and costs that arise strictly from these nonlinear contributions.

In the following section, we summarize our approach suggested by the work of Baumgarte.

Nonlinear Control Through Invariant Manifold Tracking

We base our control scheme on the notion that it is possible to force the trajectories of the nonlinear system onto selected manifolds that are prescribed as functions of the configuration variables $\boldsymbol{q}$, the generalized velocities $\boldsymbol{q}'$, and possibly the time. In actuality, these functions are imposed on the system as equality constraints having the general form

$$f(\boldsymbol{q}, \boldsymbol{q}', t) = 0 \tag{13}$$

No assumptions concerning the linearity or nonlinearity of these functions are required.

To ensure, as best we can, that the system trajectories are forced onto a constraint manifold (or manifolds), we require that the equality constraint expressed in Eq. (13) be altered as suggested by Baumgarte so that the original constraints are maintained without increasing error. These artificial constraint equations are constructed as simple linear differential equations, whose solutions are asymptotically stable to the original constraint in the independent variable. The artificial constraint equations we found useful in our analysis have the general form

$$f' + \gamma f = 0 \tag{14}$$

where $\gamma > 0$ is an arbitrary weighting function that is positive throughout the time domain of application. The solution to this equation is the expression

$$f = A \exp\left(- \int \gamma \, \mathrm{d}\tau \right) \tag{15}$$

which has the property that, as time progresses, $f \longrightarrow 0$ and the system trajectories tend to remain near the manifold specified in Eq. (13). We call this control process *invariant manifold tracking.* When we write the equations of motion appropriately, γ can be seen to function as the gain for (nonlinear) feedback control accelerations.

We have found it a straightforward process to incorporate these artificial constraints into the equations of motion by applying the second-order form of the generalized d'Alembert–Lagrange principles[8] written for m configuration variables q_r as the scalar equation

$$\sum_{r=1}^{m} \left(\Lambda_{q_r}(\mathcal{L}) - Q_r^* \right) \delta q_r'' = 0 \tag{16}$$

In this expression, $\mathcal{L}$ is the system Lagrangian, Q_r^* is the generalized nonconservative force associated with coordinate q_r, $\delta q_r''$ is a kinematically arbitrary variation of $\mathrm{d}^2 q_r / \mathrm{d}\tau^2$ that does not violate the artificial constraint equation(s) [Eq. (14)], and the Lagrange functional operator Λ is

$$\Lambda_{q_r}(\mathcal{L}) = \frac{\mathrm{d}}{\mathrm{d}\tau} \left(\frac{\partial \mathcal{L}}{\partial q_r'} \right) - \frac{\partial \mathcal{L}}{\partial q_r} \tag{17}$$

Implicit in this δ notation is the understanding that the variations of the derivatives of lower orders and that of time are zero. In terms of the configuration variables and their derivatives, the second-order d'Alembert–Lagrange variational principle provides

$$\delta q_r = \delta q_r' = \delta t = 0, \qquad r = 1, \ldots, m \tag{18}$$

Accordingly, the second-order variation of the artificial constraint relation of Eq. (14) is

$$\sum_{r=1}^{m} \frac{\partial f''}{\partial q_r''} \delta q_r'' = 0 \tag{19}$$

Solving this equation for one of the variations $\delta q_i''$ in terms of the remaining $\delta q_r''$, for $r \neq i$, provides a substitution into Eq. (16) that produces an equation whose factors $\delta q_r''$ are all linearly independent. Setting their coefficients to zero provides the constrained equations of motion. The system of m equations is completed with the addition of the artificial constraint relation of Eq. (14).

From a dynamical systems perspective, the system Hamiltonian $\mathcal{H}$ can define an invariant or constraint manifold of the chosen force model.[9] If a choice of initial conditions pertaining to a specific model results in a periodic trajectory, the Hamiltonian defines the manifold where upon this periodic solution must remain. Any unmodeled perturbations that impinge on the given system will result in a real-world deviation from the invariant manifold that was defined through the approximating equations. Actual control costs for maintaining a periodic state based on using the linear system of Hill's equations as an approximating model are not negligible. The dominant contributions from nonlinear Hill's equations are one of the many significant contributors to these costs and is the subject of our investigation.

To gain a baseline reference for the nonlinear control structure, we first apply our control method of invariant manifold tracking to the linear Hill's equations and then to the first-order nonlinear Hill's equations. We follow that development with a comparison of control costs needed to force the trajectories of the nonlinear system back onto the manifold defined by periodic solutions of the linear equations.

Control for Linear Hill's Equations

The Hamiltonian for linear Hill's equations $\mathcal{H}_\ell$ is an integral of the motion and is written

$$\mathcal{H}_\ell = \tfrac{1}{2}(x'^2 + y'^2 + z'^2) - \tfrac{1}{2}(3x^2 - z^2) \tag{20}$$

This expression will serve as the principal constraint manifold in our nonlinear control efforts. Written in the form of Eq. (13), the constraint becomes

$$f_\ell = \mathcal{H}_\ell - \mathcal{H}_{\ell_0} = 0 \tag{21}$$

where the constant $\mathcal{H}_{\ell_0}$ represents the linear Hamiltonian evaluated with the periodic initial conditions. Then, the artificial constraint is

$$f_\ell' + \gamma f_\ell = 0 \tag{22}$$

Taking the second-order variation as outlined previously gives

$$z'\delta z'' = -[x'\delta x'' + y'\delta y''] \tag{23}$$

and we consider (arbitrarily) that $\delta z''$ is the dependent variation.

In terms of our x, y, z configuration variables, the fundamental variational equation, Eq. (16) becomes

$$\Lambda_x \delta x'' + \Lambda_y \delta y'' + \Lambda_z \delta z'' = 0 \tag{24}$$

Substituting for $\delta z''$ produces a reduced fundamental equation, whose variations are linearly independent such that the coefficients of the remaining variations must satisfy

$$z'\Lambda_x - x'\Lambda_z = 0 \tag{25a}$$

$$z'\Lambda_y - y'\Lambda_z = 0 \tag{25b}$$

These are the constrained equations of motion that must be solved simultaneously along with the artificial constraint [Eq. (22)].

By algebraic rearrangement, these equations can be rewritten so that the right-hand sides function as control accelerations of the original unconstrained equations of motion. These *controlled* linear Hill's equations are

$$x'' - 2y' - 3x = -(x'/v^2)\gamma f_\ell \tag{26a}$$

$$y'' + 2x' = -(y'/v^2)\gamma f_\ell \tag{26b}$$

$$z'' + z = -(z'/v^2)\gamma f_\ell \tag{26c}$$

where f_ℓ is given in Eq. (21) and $v^2 = x'^2 + y'^2 + z'^2$.

Control for Nonlinear Hill's Equations

Our main objective is to investigate the control costs associated with controlling the nonlinear Hill's system to the constraint manifold corresponding to the Hamiltonian of the linearized Hill's equations. In this way we expect to determine the effects of the nonlinear contributions on control strategies that force the relative motion trajectories back to periodic solutions known for linear Hill's equations.

To this end, we apply the artificial constraint specified by Eq. (22) to the nonlinear Lagrangian system of Eq. (6), whose complete Hamiltonian truncated to first order is

$$\mathcal{H}_n = \tfrac{1}{2}(x'^2 + y'^2 + z'^2) - \tfrac{1}{2}(3x^2 - z^2) - \tfrac{1}{2}(2x^3 - 3xy^2 - 3xz^2) \tag{27}$$

As before, the fundamental variational equation is given by Eq. (24).

The linear dependencies among the second-order variations are the same as given in Eq. (23), producing the independent variations found in Eqs. (25). By proceeding in the same fashion as for the linear equations, using the artificial constraint of Eq. (22), we arrive at our controlled form of the first-order nonlinear Hill's equations:

$$x'' - 2y' - 3x + \tfrac{3}{2}(2x^2 - y^2 - z^2) = (x'/v^2)g \tag{28a}$$

$$y'' + 2x' - 3xy = (y'/v^2)g \tag{28b}$$

$$z'' + z - 3xz = (z'/v^2)g \tag{28c}$$

where g is given by

$$g = \tfrac{3}{2}x'(2x^2 - y^2 - z^2) - 3xyy' - 3xzz' - \gamma f_\ell \tag{29}$$

with f_ℓ given by Eq. (21) and $v^2 = x'^2 + y'^2 + z'^2$.

Numerical Testing

When we use the same initial conditions that lead to periodic linear system trajectories as described in the Introduction, the nonlinear Hill's equations, subject to the control accelerations of Eqs. (28), were compared to the linear system of Eqs. (7) to estimate ΔV requirements that minimized the along-track error. Because it is not

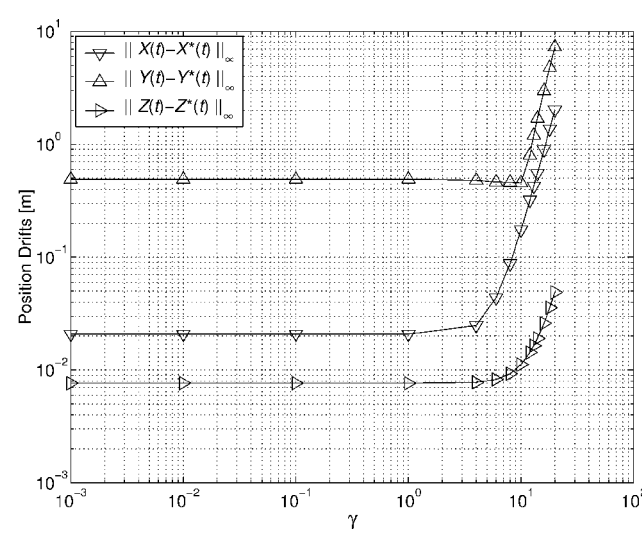

Fig. 6 Position errors ℓ_∞-norm as functions of control gain γ, one day.

generally feasible to obtain analytically an optimal gain $\gamma^{\star}$ a priori, numerical experimentation was used to determine a suitable near-optimal gain γ^{*} that produced the desired trajectories.

Figures 6–9 show the normed position differences in the search for γ^{*}, where each data point spans one day, that is, approximately 16 orbital revolutions.

As Figures 6 and 7 indicate, the near-optimal gain $\gamma^{*} = 10.80$ produces the minimum maximum along-track separation after one day. Figures 8 and 9 suggest that better overall along-track separation reduction in the ℓ_2-norm sense occurs for slightly smaller gain; however, it was decided to minimize the maximum separation over the simulation period. This is clearly done for the selected value of γ^{*}.

Figures 10–12 and Table 3 show the effect of invariant manifold tracking for the chosen gain γ^{*}. As with the uncontrolled nonlinear equations, relative position and velocity discrepancies still exist. However, we see a significant reduction in the along-track drift with the controlled equations ($\Delta Y_{\ell n^{*}}$). This drift is reduced by a factor of nearly 12 to less than 0.5 m/day.

Figure 13 shows the continuous control acceleration profiles necessary to achieve this reduction in along-track drift. The composite ΔV is seen to be roughly $8.49e{-}03$ m/s/day which, if scaled linearly, for one year would amount to slightly more than 3 m/s/year. The spiked structure of these control accelerations is encouraging

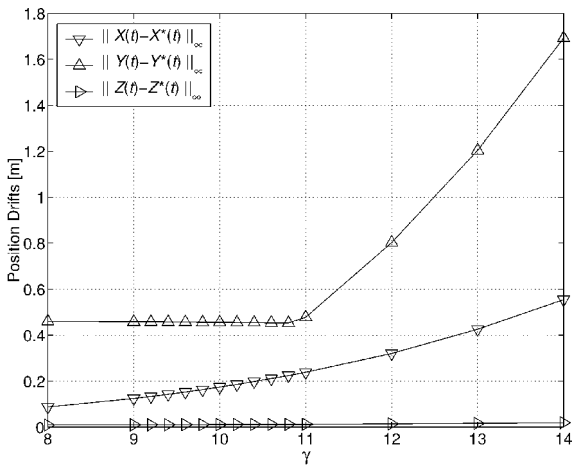

Fig. 7 Position errors ℓ_∞-norm as functions of control gain $8 \le \gamma \le 14$, one day.

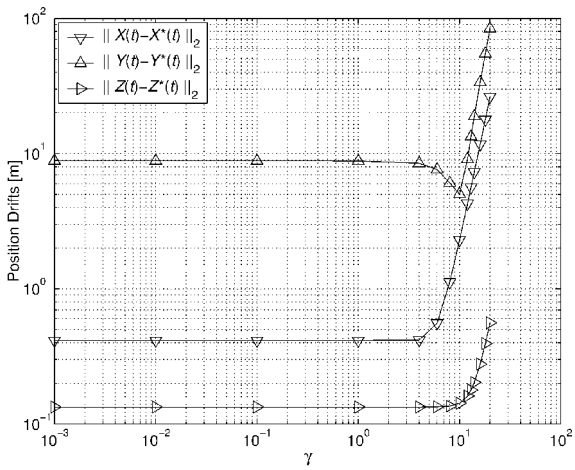

Fig. 8 Position errors ℓ_2-norm as functions of control gain γ, one day.

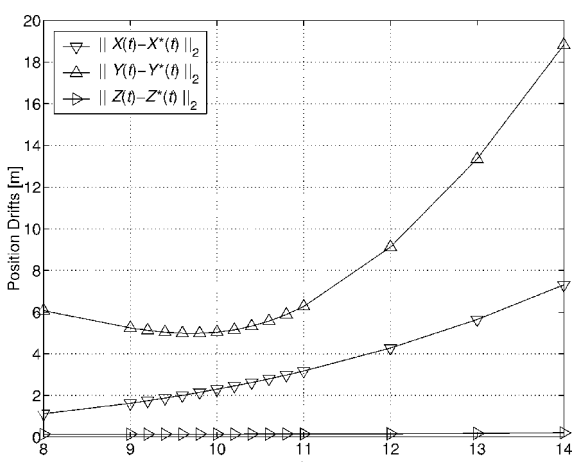

Fig. 9 Position errors ℓ_2-norm as functions of control gain $8 \le \gamma \le 14$, one day.

Table 3 Comparison of linear to controlled first-order nonlinear dynamics for one day

q	$\|q\|_2$	$\|q\|_\infty$
$\Delta X_{\ell n^{*}}$, m	2.979 309e+00	2.245 446e−01
$\Delta Y_{\ell n^{*}}$, m	5.884 058e+00	4.533 900e−01
$\Delta Z_{\ell n^{*}}$, m	1.480 689e−01	1.225 756e−02
$\Delta X'_{\ell n^{*}}$, m/s	3.331 242e−03	2.658 801e−04
$\Delta Y'_{\ell n^{*}}$, m/s	6.640 942e−03	5.653 340e−04
$\Delta Z'_{\ell n^{*}}$, m/s	2.442 324e−04	1.457 552e−05

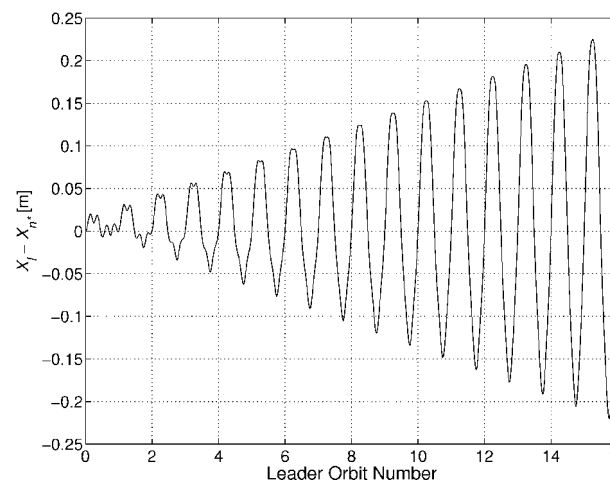

Fig. 10 Radial position difference between linear and controlled nonlinear solution with γ^{*}.

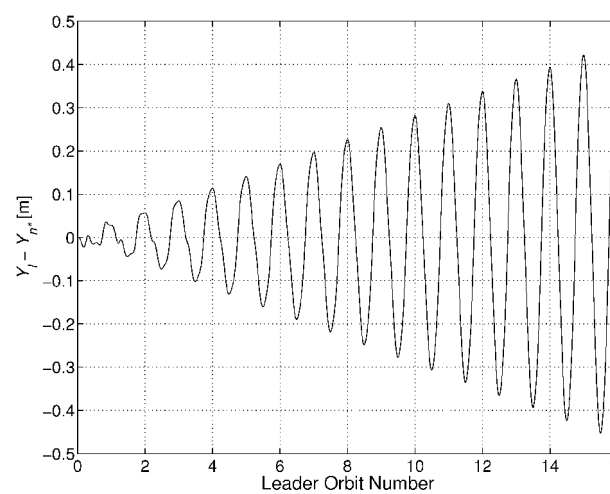

Fig. 11 Along-track position difference between linear and controlled nonlinear solution with γ^{*}.

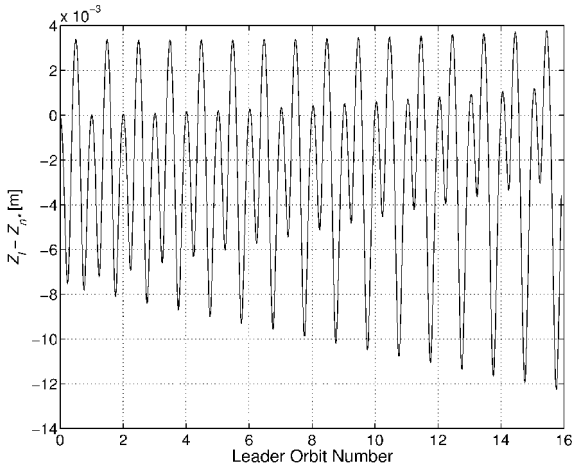

Fig. 12 Cross-track position difference between linear and controlled nonlinear solution with γ^*.

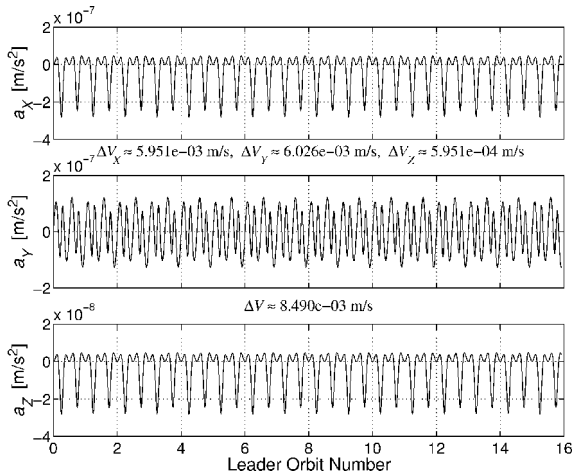

Fig. 13 Control accelerations and ΔV using linear constraint manifold with γ^*.

because they would seem amenable to a low-thrust pulse-thruster implementation. Additionally, the small magnitude of the accelerations may lend well to continuous low-thrust control, a concept that has recently seen increased interest.

Conclusions

In this paper, a useful method of controlling first-order nonlinear Hill's equations was presented. This method of invariant manifold tracking produces control accelerations that attempt to force the nonlinear system onto the invariant manifold of the linear system specified by the periodic linear system Hamiltonian. In doing so, the along-track position drift was reduced by a factor of nearly 12 using only a simple search for a desirable control gain. No a priori attempt was made to find the optimal value of the control gain.

Whereas the along-track drift rate was significantly reduced, the radial and cross-track drift and all coordinate drift rates suffered slight increases. This is not surprising since the only control objective was to minimize the maximum along-track drift during the simulation interval. As a result, a single control gain was selected for the controlled equations. There is nothing to suggest that the gain values must be identical or even constant, only that they are real and strictly nonnegative. Consequently, a second control gain could have been selected to reduce the cross-track position drift. However, this would have significantly increased the search space of adequate gains and was considered beyond the scope of this investigation.

Acknowledgments

This work was supported by the U.S. Air Force Research Laboratory and the State of Ohio through the Dayton Area Graduate Studies Institute Grant VA-UC-99-01, and a portion of this work was performed while the first named author held a National Research Council Research Associateship Award at the U.S. Air Force Research Laboratory Air Vehicles Directorate Control Theory Optimization Branch (VACA) located at Wright–Patterson Air Force Base.

References

[1]Burns, R., McLaughlin, A., Leitner, J., and Martin, M., "TechSat 21: Formation Design, Control, and Simulation," *IEEE Aerospace Conference*, Vol. 7, March 2000, pp. 19–25.

[2]Sedwick, R., Miller, D., and Kong, E., "Mitigation of Differential Perturbations in Formation Flying Satellite Clusters," *Journal of the Astronautical Sciences*, Vol. 47, Nos. 3–4, 1999, pp. 309–331.

[3]Mitchell, J., and Richardson, D., "On the In-Plane Control of Spacecraft Relative Motion," American Controls Conference, No. SHT1067, June 2001.

[4]Clohessy, W., and Wiltshire, R., "Terminal Guidance Systems for Satellite Rendezvous," *Journal of the Astronautical Sciences*, Vol. 27, No. 9, 1960, pp. 653–658.

[5]Hill, G. W., "Researches in the Lunar Theory," *American Journal of Mathematics*, Vol. 1, 1878, pp. 5–26.

[6]Baumgarte, J., "Stabilization of Constraints and Integrals of Motion in Dynamical Systems," *Computational Methods in Applied Mechanics and Engineering*, Vol. 1, No. 1, 1972, pp. 1–16.

[7]Kaplan, M. H., *Modern Spacecraft Dynamics and Control*, 1st ed., Wiley, New York, 1976.

[8]Dolaptschiew (Dolapčiev), B., "Über die verallgemeinerten Gleichungen von Lagrange und deren Zusammenhang mit dem verallgemeinerten Prinzip von d'Alembert," *Journal für die Reine und angewandte Mathematik*, Vol. 226, 1967, pp. 103–107.

[9]Goldstein, H., *Classical Mechanics*, 2nd ed., Addison–Wesley, Reading, MA, 1980, pp. 339–351.